In Vitro Cell.Dev.Biol.—Animal (2012) 48:112–122
DOI 10.1007/s11626-011-9478-4

iPSC-derived fibroblasts demonstrate augmented production and assembly of extracellular matrix proteins

Yulia Shamis · Kyle J. Hewitt · Susan E. Bear · Addy Alt-Holland · Hiba Qari · Mariam Margvelashvilli · Elana B. Knight · Avi Smith · Jonathan A. Garlick

Received: 23 November 2011 / Accepted: 21 December 2011 / Published online: 19 January 2012 / Editor: T. Okamoto

Abstract Reprogramming of somatic cells to induced pluripotent stem cells (iPSC) provides an important cell source to derive patient-specific cells for potential therapeutic applications. However, it is not yet clear whether reprogramming through pluripotency allows the production of differentiated cells with improved functional properties that may be beneficial in regenerative therapies. To address this, we compared the production and assembly of extracellular matrix (ECM) by iPSC-derived fibroblasts to that of the parental, dermal fibroblasts (BJ), from which these iPSC were initially reprogrammed, and to fibroblasts differentiated from human embryonic stem cells (hESC). iPSC- and hESC-derived fibroblasts demonstrated stable expression of surface markers characteristic of stromal fibroblasts during prolonged culture and showed an elevated growth potential when compared to the parental BJ fibroblasts. We found that in the presence of L-ascorbic acid-2-phosphate, iPSC- and hESC-derived fibroblasts increased their expression of collagen genes, secretion of soluble collagen, and extracellular deposition of type I collagen to a significantly greater degree than that seen in the parental BJ fibroblasts. Under culture conditions that enabled the self-assembly of a 3D stromal tissue, iPSC- and hESC-derived fibroblasts generated a well organized, ECM that was enriched in type III collagen. By characterizing the functional properties of iPSC-derived fibroblasts compared to their parental fibroblasts, we demonstrate that these cells represent a promising, alternative source of fibroblasts to advance future regenerative therapies.

Keywords Induced pluripotent stem cells · Human embryonic stem cells · Fibroblasts · Ascorbic acid · Extracellular matrix

Y. Shamis · K. J. Hewitt · J. A. Garlick
Program in Cell, Molecular and Developmental Biology,
Sackler School of Graduate Biomedical Sciences,
Tufts University School of Medicine,
136 Harrison Avenue,
Boston, MA 02111, USA

S. E. Bear
Department of Biology, Pine Manor College,
400 Heath Street,
Chestnut Hill, MA 02167, USA

A. Alt-Holland
Division of Cancer Biology and Tissue Engineering, Department of Endodontics, School of Dental Medicine, Tufts University,
136 Harrison Avenue, South Cove Bldg, Room 116,
Boston, MA 02111, USA

H. Qari · M. Margvelashvilli · E. B. Knight · A. Smith · J. A. Garlick (✉)
Division of Cancer Biology and Tissue Engineering,
Department of Oral and Maxillofacial Pathology,
School of Dental Medicine, Tufts University,
136 Harrison Avenue, South Cove Bldg, Room 116,
Boston, MA 02111, USA
e-mail: Jonathan.Garlick@tufts.edu

Introduction

As stromal constituents of many tissues, fibroblasts play an essential role in regulating normal tissue homeostasis and wound repair through their synthesis of extracellular matrix (ECM) proteins and secretion of growth factors. The composition and organization of ECM produced by stromal fibroblasts direct many aspects of cell behavior including growth, survival, cell recruitment, and differentiation during tissue repair and regeneration (Schultz and Wysocki 2009). Incorporation of stromal fibroblasts into tissue-engineered biomaterials has shown great promise for their application in regenerative medicine to replace damaged or diseased

tissues by fabricating skin and dermal substitutes (Wong et al. 2007), tendon and ligament tissue replacements (Gurkan et al. 2010), corneal tissues (Proulx et al. 2010), heart valves (Schmidt and Hoerstrup 2006), and blood vessels (Grainger and Putnam 2011). However, the therapeutic potential of stromal fibroblasts has been limited by our incomplete understanding of the precursor cells that give rise to them and by their phenotypic heterogeneity (Chang et al. 2002; Sorrell and Caplan 2004; Phan 2008). In addition, the lack of specific markers defining functional subpopulations of stromal fibroblasts has complicated their characterization for potential use in regenerative therapies (Yamaguchi et al. 1999; Koumas et al. 2001; Haniffa et al. 2007; Sorrell et al. 2007, 2008). In light of this, next-generation treatment strategies in tissue repair will require the use of novel sources of fibroblasts that can offer more defined progenitor populations and more predictable tissue outcomes upon their therapeutic use.

Human induced pluripotent stem cells (iPSC) offer a novel source of autologous cells for therapeutic use (Klimanskaya et al. 2008). Following their reprogramming from a variety of somatic cell types, iPSC can be differentiated into patient-specific cells with a wide spectrum of cellular phenotypes (Lian et al. 2007; Swistowski et al. 2010; Liu et al. 2011). Specifically, several recent studies (Xu et al. 2004; Stojkovic et al. 2005) and previous work in our laboratory (Hewitt et al. 2009) have shown the derivation of cells with properties of stromal fibroblasts from both, human embryonic stem cells (hESC) and from iPSC. Such fibroblasts have been used as autogenic feeders to support the culture of undifferentiated hESC (Xu et al. 2004; Stojkovic et al. 2005) and have been shown to secrete paracrine factors that direct the normal development and repair of engineered, 3D human skin equivalents (Hewitt et al. 2011; Shamis et al. 2011). Recently, evidence has emerged that fibroblasts differentiated from iPSC displayed specific properties that exceeded those of the parental fibroblasts from which these iPSC were originally reprogrammed. For example, iPSC-derived fibroblasts showed an extended replicative potential (Suhr et al. 2009; Lapasset et al. 2011) and improved mitochondrial function (Suhr et al. 2010; Lapasset et al. 2011) when compared to the parental fibroblasts used for iPSC reprogramming. In addition, mesenchymal stem cells (MSC) derived from iPSC showed improved rescue of limb ischemia when compared to adult-derived MSC (Lian et al. 2010). This suggests that the biological potential of iPSC-derived cells may be augmented following cellular reprogramming and subsequent differentiation to a specific cell type. However, it is not yet known if fibroblasts differentiated from iPSC can also demonstrate improved functional features that may be beneficial for regenerative therapies when compared to the parental fibroblasts from which these iPSC were initially reprogrammed.

In this study, we have compared the production and assembly of ECM by iPSC-derived fibroblasts (iPDK) to that of stromal, foreskin fibroblasts (BJ), the parental cells from which these iPSC were initially reprogrammed. We found that in the presence of L-ascorbic acid-2-phosphate (AA), iPSC-derived fibroblasts expressed elevated levels of ECM proteins that exceeded the amounts produced by BJ fibroblasts, yet were very similar to control fibroblasts that were differentiated from hESC (EDK). Stimulation with AA increased the secretion of soluble collagen and elevated the deposition of type I collagen in 2D monolayer culture in both, iPDK and EDK fibroblasts when compared to BJ. Under culture conditions that enabled the organization of a 3D ECM, iPDK and EDK fibroblasts demonstrated the capacity to assemble a well-organized, stroma-like tissue by depositing elevated amounts of ECM when compared to BJ fibroblasts. Immunoblot and imunohistochemical analysis of the composition of these stromal tissues revealed that ECM assembled by both, iPDK and EDK fibroblasts contained significantly greater amounts of type III collagen than that assembled by BJ. These data demonstrate that fibroblasts differentiated from iPSC acquired an augmented biological potency when compared to their parental fibroblasts as characterized by their increased production and assembly of ECM, functional features important for application of these cells in regenerative therapies.

Materials and Methods

Cell lines. BJ fibroblasts were purchased from ATCC Inc. (Manassas, Virginia) and expanded on tissue culture plastic in DMEM (Invitrogen, Carlsbad, CA) supplemented with 10% FBS (Hyclone, Logan, UT). The iPSC line (gift of the lab of Dr. Konrad Hochedlinger, Boston, MA) (Maherali et al. 2008), was derived by reprogramming BJ fibroblasts using separate dox-inducible vectors Oct4, Sox2, Klf4, cMyc, and Nanog. The H9 line of hESC was purchased from the WiCell Institute (Madison, WI). All patient-derived cells used for this study were derived from anonymous donors and are not identifiable, and thus are exempt from IRB approval. The iPSC and the hESC lines were maintained in culture as previously described (Thomson et al. 1998). EDK and iPDK fibroblast cell lines were differentiated from hESC and iPSC, respectively, using our previously described protocol for the generation of fibroblasts (Hewitt et al. 2009; Hewitt et al. 2011). For all experiments, BJ, EDK, and iPDK cell lines were grown on type I collagen-coated plates (BD Biosciences, San Jose, CA) in media consisting of 3:1 DMEM/F12 (Invitrogen, Carlsbad, CA), 5% FCII (Hyclone, Logan, UT), 0.18 mM adenine, 8 mM HEPES, 0.5 μg/mL hydrocortisone, 10^{-10} M cholera toxin, 10 ng/mL EGF, 5 μg/mL insulin (all from Sigma, St.

Louis, MO). All cell lines were routinely checked for mycoplasma contamination using MycoAlert® Mycoplasma detection kit (Lonza, Rockland, ME).

Proliferation kinetics. BJ, EDK, and iPDK fibroblasts of the same passage (p8) underwent additional passaging every 7 days upon reaching 70–80% confluence. Cell numbers were determined by counting trypsinized cells using a hemocytometer, and data were recorded as an average of three measurements for each passage. As cell numbers were first determined at p8, the number of population doublings (PD) was first calculated for p9 using the following formula: $X = [\log10(N_H) - \log10(N_1)]/\log10(2)$. The N_H is the harvested cell number and the N_1 is the plated cell number. The PD for each passage was calculated and added to the PD of the previous passages to calculate the cumulative population doublings.

Real-time RT-PCR. RNA was isolated using Qiagen RNeasy purification kit (Qiagen, Valencia, CA), and then converted to cDNA with the iScript cDNA synthesis kit (Biorad, Hercules, CA) using 0.5 μg RNA. Real-time RT-PCR reactions were carried out using 20 ng of cDNA, 200nM of each primer, and 2× SYBRgreen Supermix (Biorad, Hercules, CA) at a total sample volume of 12.5 μL and samples were run in triplicate on a iQ5 Real-Time PCR detection system (Bioad, Hercules, CA). PCR products were amplified to 30 cycles at 94°C for 30 s, 60°C for 30 s, and 72°C for 60 s. The relative level of gene expression was assessed using the $2^{-\Delta\Delta C}$t method. Error bars represent standard deviation of three biological replicates. The following oligonucleotide primer sequences were used: GAPDH-F: 5′-tcgacagtcagccgcatcttcttt-3′, GAPDH-R: 5′-accaaatccgttgacctt-3′; COL1A1-F: 5′-cctcctgacgcacggccaag-3′, COL1A1-R: 5′-ccctcgacgccggtggtttc-3′: COL3A1-F: 5′-cctccaactgctcctactcg-3′, COL3A1-R: 5′-tcgaagcctctgtgtcctttt-3′; COL4A1-F: 5′-ccaggatttcaaggtccaaa-3′, COL4A1-R: 5′-tcattgccttgcacgtagag-3′; COL5A1-F: 5′-ctggggagaaggg aaaactc-3′, COL5A1-R: 5′-tcagtccaagagctcccact-3′; FN-F: 5′-tgaccctacagtttccca-3′, FN-R: 5′-tgattcagacattcgttcccac-3′.

Histology, immunohistochemistry, and immunofluorescence. Self-assembled, 3D stromal tissues were fixed in 10% neutral-buffered formalin, embedded in paraffin, sectioned at 8 μm thickness and hematoxylin and eosin (H&E) staining was performed to assess tissue morphology. For immunohistochemistry, antigen retrieval was performed by steaming tissue sections in citrate buffer for 15 min and immunostaining was performed with antibodies against type I collagen, type III collagen (Abcam, Cambridge, MA), and fibronectin (BD Transduction, San Jose, CA). Staining localization was detected using DAB (Vector Laboratories, Burlingame, CA), and tissues were counterstained with hematoxylin (Sigma, St. Louis, MO). For immunofluorescence staining, BJ, EDK, and iPDK cells were grown in 2D, monolayer cultures on glass cover slips for 1 wk in the presence or absence of AA (10 μg/ml), fixed in 4% paraformaldehyde, permeabilized using 0.1% triton X-100, immunostained with antibodies against type I procollagen (Fitzgerald Inc, Acton, MA). Staining localization was detected using Alexa Fluor 488-conjugated goat anti-mouse secondary antibody (Invitrogen, Carlsbad, CA). Microscopy was performed with a Nikon Eclipse 80i microscope and composite images were created using SPOT Advanced software (Diagnostic Instruments, Sterling Heights, MI).

Construction of 3-dimensional (3D) stromal tissues. BJ, EDK, and iPDK cells were harvested at 70–80% confluence and seeded onto 24-well Millicell® (Millipore, Billerica, MA) Hanging Cell Culture inserts (1.0-μm pore size) at a density of 5×10^5 cells/cm^2. Cells were fed with the media containing 3:1 DMEM/F12 (Invitrogen, Carlsbad, CA), 5% FCII (Hyclone, Logan, UT), 0.18 mM adenine, 8 mM HEPES, 0.5 μg/mL hydrocortisone, 10^{-10} M cholera toxin, 10 ng/mL EGF, 5 μg/mL insulin with or without 10 μg/ml of L-ascorbic acid-2-phosphate (Sigma, St. Louis, MO) and medium was changed every 3 d throughout the culture period of 5 wk.

Flow cytometry. BJ, EDK, and iPDK cells were trypsinized, pelleted, and re-suspended in 2% FBS in PBS. Cell suspensions were stained with PE-conjugated anti-CD73, CD10, CD90, CD166, or isotype control IgG1k (BD Pharmingen, San Jose, CA). Cells were incubated for 30 min on ice and washed with 2% FBS in PBS solution. All data were acquired using a FACSCalibur (BD, San Jose, CA) and analyzed using CellQuest (BD, San Jose, CA) and Summit V4.3 software (Dako, Carpentaria, CA). Analysis was performed on 20,000 cells per sample and positive expression was defined as the level of fluorescence greater than 99% of the corresponding isotype control IgG1k (BD Biosciences, San Jose, CA).

Immunoblotting. BJ, EDK, and iPDK cells were grown for 1 week in monolayer culture in the presence or absence of AA (10 μg/ml). 3D stromal tissues were grown for 5 wk in the presence of AA (10 μg/ml). Proteins were extracted on ice in 4% deoxycholate (4% sodium deoxycholate in 20 mM Tris–HCl pH 8.8, protease and phosphatase inhibitors) followed by five rounds of sonication. Extracts were spun down at 14,000 rpm for 30 min at 4°C and protein concentrations were determined using NanoDrop2000 (Thermo Scientific, Wilmington, DE). Equal protein samples were separated by SDS-PAGE (4–20% gel) under non-reducing conditions (type I collagen and type III collagen) and reducing conditions (fibronectin). Proteins were transferred to nitrocellulose membranes in 20% methanol in running buffer. Membranes were immunoblotted with antibodies against type I collagen and type III collagen (Abcam, Cambridge, MA), fibronectin (BD

Transduction, San Jose, CA) and ERK 1/2 (Santa Cruz Biotechnology, Santa Cruz, CA). HRP-conjugated secondary antibodies were from Jackson ImmunoResearch Laboratories (West Grove, PA). Densitometry analysis of scanned blots was performed using ImageJ software (U. S. National Institutes of Health, Bethesda, MD).

Soluble collagen assay. BJ, EDK, and iPDK 0.5×10^5 cells were seeded onto 100-mm culture dishes and maintained in 10 ml of tissue culture medium with and without AA (10 μg/ml) for 1 week. Before analysis, cells were fed with fresh growth medium for the final 48 h of their incubation. For measurement of soluble collagens, tissue culture supernatants were collected and analyzed by Sircol™ assay (Biocolor, Ireland) according to the manufacturer's protocol. Assays were performed in triplicate from three independent samples. Absorbance was read at 540 nm using a plate reader and the concentrations of soluble collagen were determined from a standard curve that was generated using rat tail collagen provided by the manufacturer.

Data analysis. Results of our analysis were expressed as mean±SD of at least three independent samples. Statistical comparisons between groups were performed with a two-tailed Student's *t* test, $*P\leq0.05$ and $**P\leq0.01$ were considered significant.

Results

iPSC-derived cells demonstrate fibroblast morphology following extended culture and show prolonged growth potential when compared to parental BJ fibroblasts. Fibroblast cell lines were generated from the H9 line of hESC (EDK) and from iPSC (iPDK) that were initially reprogrammed from BJ fibroblasts using our previously established differentiation protocol (Hewitt et al. 2009; Hewitt et al. 2011). Upon long-term expansion, iPDK and EDK cell lines maintained a stable, mesenchymal morphology that was very similar to the morphology of BJ fibroblasts (Fig. 1*A*). Characterization of the growth kinetics of these cells revealed significant differences between these cell lines, as demonstrated by their cumulative growth curves (Fig. 1*B*). In vitro expansion potential of iPDK, BJ and control EDK fibroblasts was assessed by calculating population doublings (PDs) during serial subculture. All three cell lines were thawed at passage 8 and subcultured weekly over a period of 3 mo. As illustrated in Fig. 1*B*, EDK, iPDK, and BJ fibroblasts demonstrated very similar PDs until passage 12. The decline in PDs of BJ fibroblasts first occurred at passage 13 (mean PDs at p13: BJ=1.8±0.6, iPDK=3.5±0.7, EDK=3.6±0.2) followed by loss of growth potential at passage 16 (mean PDs at p16: BJ=0.2±0.2, iPDK=2.2±0.1, EDK=3.3±0.4). The cultures were considered to have lost their growth potential when cells underwent less than one PD per passage. The decline in PDs of iPDK and EDK cells was seen after passages 16 and 19, respectively (mean PDs at p19: BJ=0.2±0.06, iPDK=0.07±0.07, EDK=2.6±0.07). Loss of growth potential of iPDK fibroblasts occurred at passage 19, while EDK fibroblasts continued to proliferate beyond the 20th passage. These results demonstrated that the growth of both hESC- and iPSC-derived fibroblasts was markedly prolonged when compared to BJ fibroblasts.

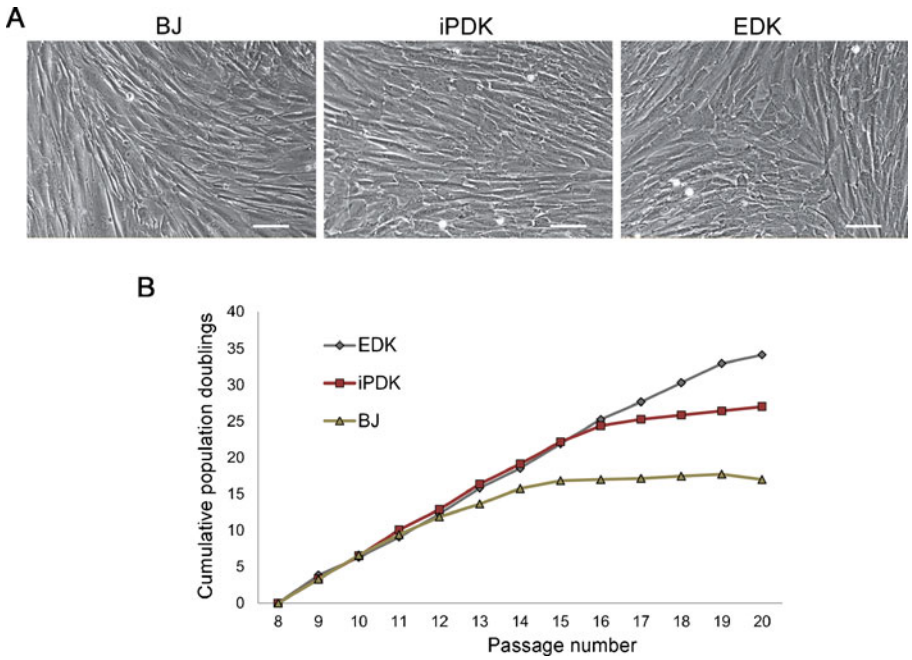

Figure 1. Characterization of morphology and growth potential of iPSC-derived fibroblasts, hESC-derived fibroblasts, and parental BJ fibroblasts. (*A*) Fibroblasts differentiated from iPSC (*iPDK*) demonstrated typical fibroblast morphology that was similar to foreskin-derived, stromal fibroblasts (*BJ*), and control fibroblasts differentiated from hESC (*EDK*). *Bar*, 50 μm. (*B*) Growth capacity of *iPDK*, *BJ*, and control *EDK* fibroblasts was assessed by calculating cumulative population doublings during serial subculture. EDK and iPDK fibroblasts demonstrated increased growth potential when compared to BJ fibroblasts.

iPSC-derived fibroblasts express elevated levels of genes for ECM proteins when compared to BJ fibroblasts. Production of extracellular matrix (ECM) proteins is an essential feature of stromal fibroblast function that is needed for tissue maintenance and repair. As it is known that L-ascorbic acid-2-phosphate (AA) promotes the deposition and organization of ECM proteins by stromal fibroblasts (Murad et al. 1981; Chojkier et al. 1989), we sought to determine whether iPSC- and hESC-derived fibroblasts were also responsive to AA. To address this, we performed quantitative real-time RT-PCR to measure expression levels of ECM proteins in iPDK, BJ, and control EDK fibroblasts after growth for 1 week in the presence or absence of AA. We observed significantly greater AA responsiveness and expression of genes for ECM proteins in both iPDK and EDK cells when compared to BJ fibroblasts (Fig. 2). Stimulation with AA (10 μg/ml) had little or no effect on expression of pro-α1(I) collagen (COL1A1) and pro-α1(IV) collagen (COL4A1) in BJ fibroblasts, while expression of pro-α1(III) collagen (COL3A1) and pro-α1(V) collagen (COL5A1) were increased 3- and 5-fold, respectively. When stimulated with AA, iPDK cells demonstrated a 2-fold increase in COL1A1, a 3-fold increase in COL3A1, an 8-fold increase in COL4A1, and a 35-fold increase in COL5A1 mRNA levels when compared to cells not stimulated with AA. Similar to iPSC-derived fibroblasts, hESC-derived fibroblasts also expressed elevated levels of collagen precursors in response to AA. When stimulated with AA, EDK cells demonstrated a 5-fold increase in COL1A1, 15-fold increase in COL3A1, 6-fold increase in COL4A1, and 125-fold increase in COL5A1 mRNA levels. Stimulation with AA had a negligible effect on expression of the non-collagenous ECM protein, fibronectin (FN), in all three cell lines. However, the baseline expression levels of FN were noticeably higher in both, iPDK and EDK cells when compared to BJ fibroblasts. These findings demonstrated that both hESC- and iPSC-derived fibroblasts were responsive to AA, which elevated the expression of collagen genes to a significantly greater degree than those seen in BJ fibroblasts.

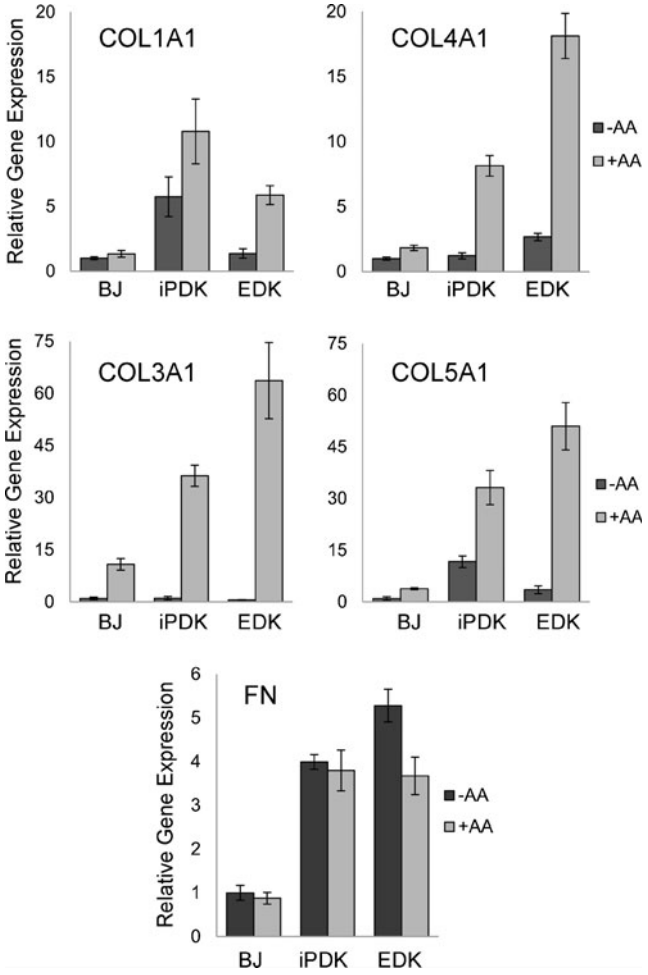

Figure 2. Fibroblasts differentiated from iPSC and hESC expressed elevated levels of collagenous proteins in the presence of ascorbic acid that exceeded those expressed by the parental BJ fibroblasts. Real-time RT-PCR analysis of ECM proteins showed that EDK and iPDK fibroblasts expressed elevated levels of proα1(I) collagen (*COL1A1*), proα1(III) collagen (*COL3A1*), proα1(IV) collagen (*COL4A1*), and proα1(V) collagen (*COL5A1*) when compared to BJ fibroblasts in the presence of L-ascorbic acid-2-phosphate (*AA*). AA stimulation had no effect on expression of fibronectin (*FN*). Results represent the mean expression levels normalized to GAPDH; *error bars* represent SD from three independent experiments.

iPSC-derived fibroblasts respond to ascorbic acid stimulation by increasing collagen secretion and extracellular deposition to a greater degree than parental BJ fibroblasts. We compared the potential of iPDK, BJ, and control EDK fibroblasts to secrete, process, and deposit collagen using a soluble collagen assay, immunofluorescence staining, and Western blot analysis. Fibroblasts were cultured for 1 wk in the presence or absence of AA, and supernatants were collected after 48 h of incubation to measure levels of total soluble collagen (types I–V collagen) using Sircol™ assay (Fig. 3*A*). BJ fibroblasts showed reduced levels of soluble collagen protein as compared to iPDK and EDK fibroblasts. In the presence of AA, all three cell types showed significantly elevated levels of total soluble collagen when compared to cells grown in the absence of AA (*$P \leq 0.05$, **$P \leq 0.01$). However, AA increased the production of total soluble collagen to a greater extent by EDK and iPDK cells (238±28% in EDK and by 142±17% in iPDK vs. untreated control) when compared to BJ fibroblasts (by 26±4% in BJ vs. untreated control). To determine whether AA increased deposition of extracellular collagen, we performed immunofluorescence staining to compare the localization of type I procollagen in iPDK, BJ, and control EDK fibroblasts that were grown in 2D monolayer cultures in the presence or absence of AA (Fig. 3*B*). In the absence of AA, all three cell types demonstrated a similar cytoplasmic

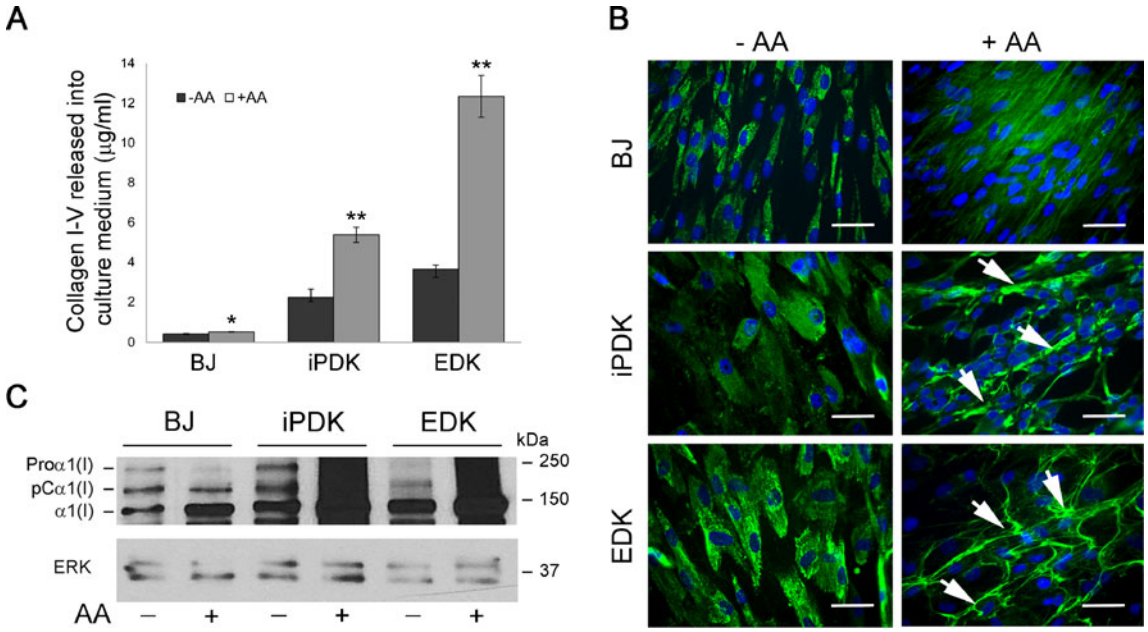

Figure 3. Stimulation with ascorbic acid induces secretion and deposition of collagenous proteins in iPSC- and hESC-derived fibroblasts to a greater degree than BJ fibroblasts. (*A*) Soluble collagen assay (Sircol™) showed that AA induced higher secretion levels of collagens I–V in EDK and iPDK than in BJ fibroblasts (*t* test: $*P<0.01$, $**P<0$) compared to untreated controls. Results represent the mean±SD of three measurements from three independent experiments. (*B*) Immunofluorescence analysis of type I procollagen localization in *EDK*, *iPDK*, and *BJ* cells grown in the presence or absence of AA. In the presence of AA, EDK and iPDK fibroblasts deposited higher amount of type I procollagen into the extracellular space between cells (*arrows*, *B*) than BJ fibroblasts. *Bars*, 50 µm. (*C*) Western blot analysis of type I collagen demonstrated that conversion of proα1(I) collagen to the mature α1(I) form was more efficient in the presence of AA in all three cell types. However, AA increased production of α1(I) collagen to a greater extent in EDK and iPDK cells than in parental BJ fibroblasts.

localization of type I procollagen without extracellular deposition. In the presence of AA, both, iPDK and EDK cells demonstrated elevated accumulation of type I procollagen in the extracellular space when compared to type I procollagen deposited by BJ fibroblasts (Fig. 3*B*, arrows). To determine if stimulation with AA increased processing of proα1(I) collagen in EDK and iPDK cells, we performed Western blot analysis using an anti-collagen I antibody that recognizes all three forms of α1(I) collagen: the unprocessed procollagen α1(I) chain (Proα1(I)), the C-terminal procollagen α1(I) chain (pC-α1(I)), and the fully processed α1(I) chain with both the N- and C- propeptides cleaved (α1(I)). Immunoblots showed that in the presence of AA, the generation of mature α1(I) collagen was more efficient in all three cell types (BJ, iPDK, and EDK), as seen by the loss of the Proα1 (I) band which likely reflects AA-stimulated hydroxylation of proline and lysine residues in procollagen (Fig. 3*C*). However, in the presence of AA, EDK, and iPDK cells generated significantly greater amount of α1(I) collagen when compared to BJ fibroblasts (Fig. 3*C*). Taken together, these results demonstrated that iPSC-derived fibroblasts showed elevated secretion and extracellular deposition of collagen when compared to BJ fibroblasts, yet were similar to levels produced by hESC-derived fibroblasts.

Deposition and organization of ECM proteins in 3D self-assembled, stroma-like tissues are increased in iPSC-derived fibroblasts when compared to their parental BJ fibroblasts. Since AA induced an increase in production and deposition of ECM proteins in iPDK and EDK fibroblasts in 2D monolayer culture, we next assessed the potential of iPDK, BJ, and control EDK fibroblasts to deposit and organize a 3D ECM under conditions that enabled assembly of a stroma-like tissue. These three cell types were seeded at high density on a porous polycarbonate membrane in a transwell and cultured for 5 weeks in the presence or absence of AA. In this way, it was possible to assess the production and assembly of ECM produced by EDK, iPDK, and BJ fibroblasts under more stringent experimental conditions than in 2D monolayer culture. Tissues harboring each of these three cell types were examined for the degree to which they could organize stromal architecture and for thickness of tissues generated upon assembly of 3D ECM. Histological analysis of these tissues demonstrated the presence of fibroblasts aligned in a dense collagenous matrix (Fig. 4*A*, inserts). Tissue constructs assembled by BJ fibroblasts showed a more fibrillar connective tissue that was less compact compared to those assembled by iPDK and EDK cells (Fig. 4*A*). To quantify differences in the amount of ECM produced by these cell lines in these tissues, we measured the thickness

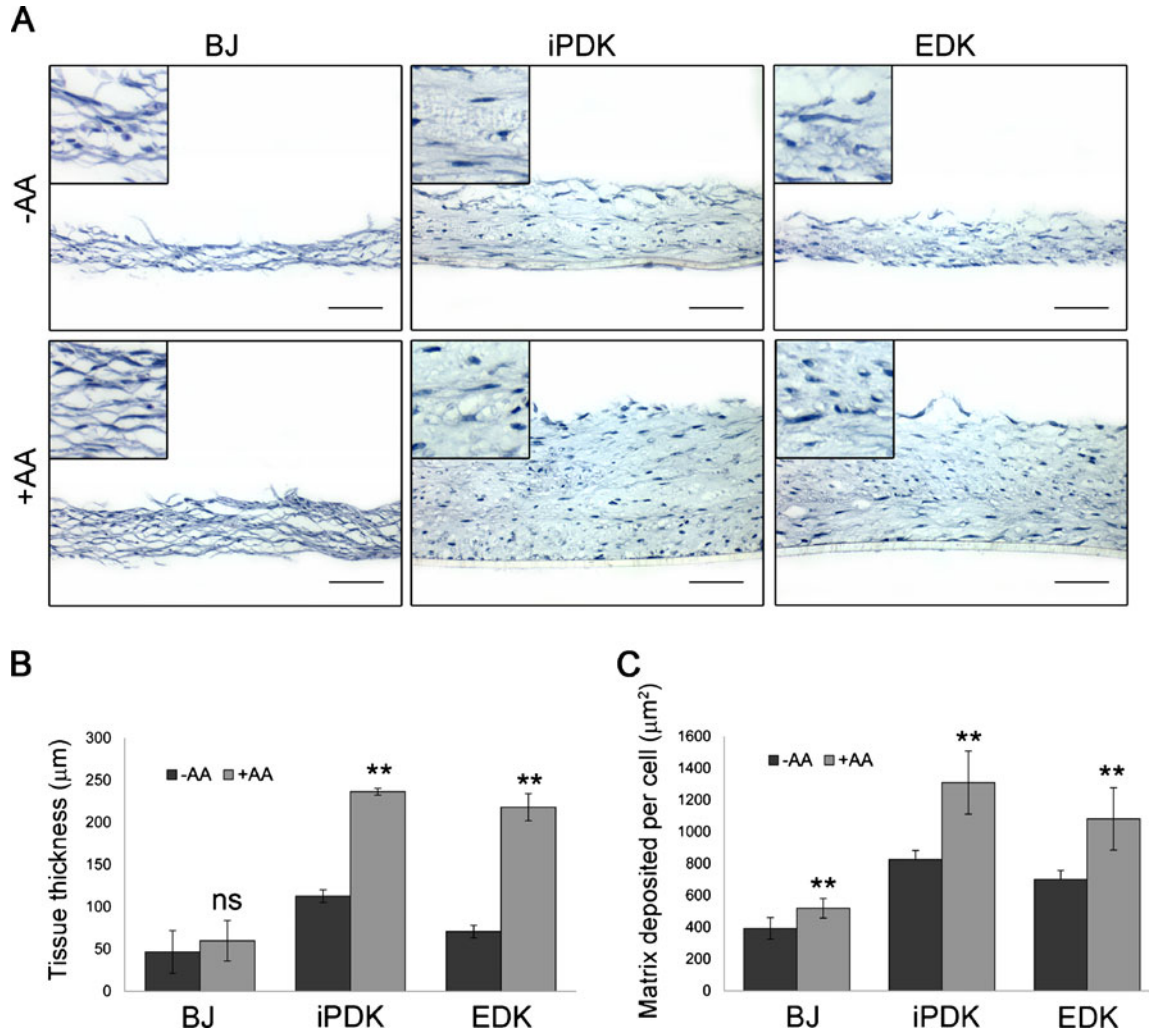

Figure 4. hESC- and iPSC-derived fibroblasts assemble a 3D ECM that is thicker and more organized than that produced by BJ fibroblasts. (*A*) Representative H&E stains of tissue constructs assembled by *BJ*, *iPDK*, and *EDK* fibroblasts. *Bars*, 100 μm. (*B*) Measurements of tissue thickness showed that iPDK and EDK fibroblasts assembled significantly thicker tissues than BJ fibroblasts in both the presence and absence of AA (*t* test: $^{**}P<0.01$). (*C*) Quantification of ECM deposition on a per cell basis showed that stimulation with AA increased ECM deposition and assembly in all three cell types (*t* test: $^{**}P<0.01$). However, the capacity of AA to increase deposition of ECM was greater in iPDK and EDK than BJ fibroblasts. Results represent the mean±SD from three independent experiments, three sections per each tissue.

and the amount of ECM deposited on a per cell basis using multiple sections from three independent experiments. Tissue thickness measurements revealed that iPDK and EDK fibroblasts assembled significantly thicker tissues than BJ fibroblasts when grown in the presence of AA (Fig. 4*B*). To quantify the amount of ECM deposited on a per cell basis in each construct, we measured the area of each tissue that was normalized to the number of cells present (Fig. 4*C*). These measurements demonstrated that significantly greater amounts of ECM were deposited and assembled when all cell types were grown in the presence of AA. However, the addition of AA to EDK and iPDK cells increased ECM deposition to a greater extent (by 54±28% in EDK and by 59±24% in iPDK vs. untreated control) than was seen for BJ fibroblasts (by 32±15% in BJ vs. untreated control). To ensure that no changes occurred in the mesenchymal phenotype of EDK, iPDK and BJ fibroblasts as the result of prolonged growth conditions and exposure to AA, we used flow cytometric analysis to characterize the CD surface antigen profile of these cells after growth in 2D monolayer cultures in the absence or presence of AA for 3 and 5 wk (Table 1). All three cell lines showed stable morphology and expression of CD markers (CD90, CD73, CD10, and CD166), known to be characteristic of stromal fibroblasts. These surface markers were found in greater than 90% of EDK, iPDK, and BJ cells grown in the presence and absence of AA, indicating that neither prolonged time in culture nor exposure to AA resulted in the selection of subpopulations

Table 1. Stable expression of CD markers characteristic of stromal fibroblasts are seen in long-term culture of BJ, iPDK, and EDK by flow cytometric analysis

Cell type	Surface marker	3 weeks		5 weeks	
		−AA	+AA	−AA	+AA
BJ	CD73	98	99	97	99
	CD90	98	97	99	98
	CD10	98	99	99	99
	CD166	91	97	93	87
iPDK	CD73	97	97	97	98
	CD90	97	96	95	94
	CD10	97	97	96	94
	CD166	93	94	91	94
EDK	CD73	91	99	98	98
	CD90	99	97	99	99
	CD10	99	98	99	99
	CD166	99	93	98	98

BJ, iPDK, and EDK fibroblasts maintained stable mesenchymal phenotype when cultured over prolong period of time (up to 5 wk) in the presence of AA as shown by the expression of CD markers characteristic of stromal fibroblasts.

The percentage of cells positive for the cell surface markers are shown, each experiment is normalized to isotype control and has been repeated at least two times.

linked to a loss of fibroblast properties. These data demonstrate that fibroblasts differentiated from iPSC acquired an augmented biological potency, as seen by their increased production and assembly of ECM when compared to the BJ fibroblasts from which these iPSC were originally derived.

ECM assembled by iPSC-derived fibroblasts is enriched in type III collagen when compared to ECM produced by parental BJ fibroblasts. In addition to overall matrix production, it is known that the organization and structure of stromal tissues is dependent on the levels of production of individual ECM proteins (Sottile et al. 2007). To further compare the composition of 3D, stromal tissues assembled by EDK, iPDK, and BJ fibroblasts, we analyzed levels of type I collagen (COL1), type III collagen (COL3) and fibronectin (FN) by immunoblot and immunohistochemical analysis (Fig. 5). These tissue constructs were solubilized and subjected to Western blot analysis, which revealed that levels of both COL1 and FN were approximately 40% higher in tissues assembled by iPDK and EDK fibroblasts when compared to tissues assembled by BJ fibroblasts (Fig. 5*A–C*). Western blot analysis of COL3 demonstrated that tissues assembled by iPDK and EDK fibroblasts contained approximately 25-fold and 40-fold higher levels of COL3, respectively, when compared with tissues assembled by BJ fibroblasts (Fig. 5*A* and *D*). The presence of COL1, COL3, and FN was further verified by immunohistochemistry (Fig. 5*E*). Similar to neonatal human skin, COL1 and FN were present throughout the tissues assembled by all three cell types (BJ, iPDK, and EDK). Consistent with Western blot analysis, COL3 was detected in tissues assembled by iPDK and EDK fibroblasts but not in tissues assembled by BJ fibroblasts (Fig. 5*E*). Since COL3 is the major ECM component in the granulation tissue of healing wounds, these findings suggest that the elevated levels of COL3 in tissues harboring iPDK cells were due to the acquisition of an augmented phenotype needed for tissue repair following reprogramming of BJ cells and their subsequent differentiation to fibroblasts.

Discussion

Fibroblasts represent a diverse population of mesenchymal stromal cells that play an essential role in regulating normal tissue homeostasis and wound repair (Schultz and Wysocki 2009). However, the utility of these cells for wound repair therapy has been limited by difficulties to acquire sufficient numbers of donor cells upon ex vivo expansion and by their heterogeneity that leads to unpredictable clinical outcomes (Koumas et al. 2001; Sorrell and Caplan 2004; Sorrell et al. 2007; Wong et al. 2007; Phan 2008). In this light, the development of approaches aimed at generating clinically relevant quantities of fibroblasts with significant repair potential from pluripotent stem cells, such as iPSC, may provide plentiful and reliable alternative sources of fibroblasts for tissue repair and regeneration. In this study, we have begun to explore the potential of iPSC-derived fibroblasts for such therapeutic applications by comparing the production and assembly of ECM by iPSC-derived fibroblasts to those of the parental fibroblasts (BJ) from which iPSC were initially reprogrammed. We have found that iPSC-derived fibroblasts exceeded the growth potential of their parental BJ fibroblasts and showed an augmented capacity to deposit collagen proteins in 2D monolayer culture and to organize and assemble a 3D stroma-like tissue.

To accomplish this, we compared foreskin-derived, BJ fibroblasts to fibroblasts derived from iPSC (iPDK) and hESC (EDK) by growing these cells in 2D monolayer culture and as 3D tissues in the presence of L-ascorbic acid-2-phosphate (AA). AA is known to increase collagen synthesis by stimulating transcription of collagen genes and by acting as co-factor in post-translational procollagen hydroxylation that is essential for the stabilization of collagen triple helical structure (Peterkofsky 1972; Murad et al. 1981; Chojkier et al. 1989). In addition, it has been found that dermal fibroblasts exposed to AA can assemble stroma-like tissues, composed of a multilayer of fibroblasts surrounded by dense accumulations of mature collagen fibrils in the

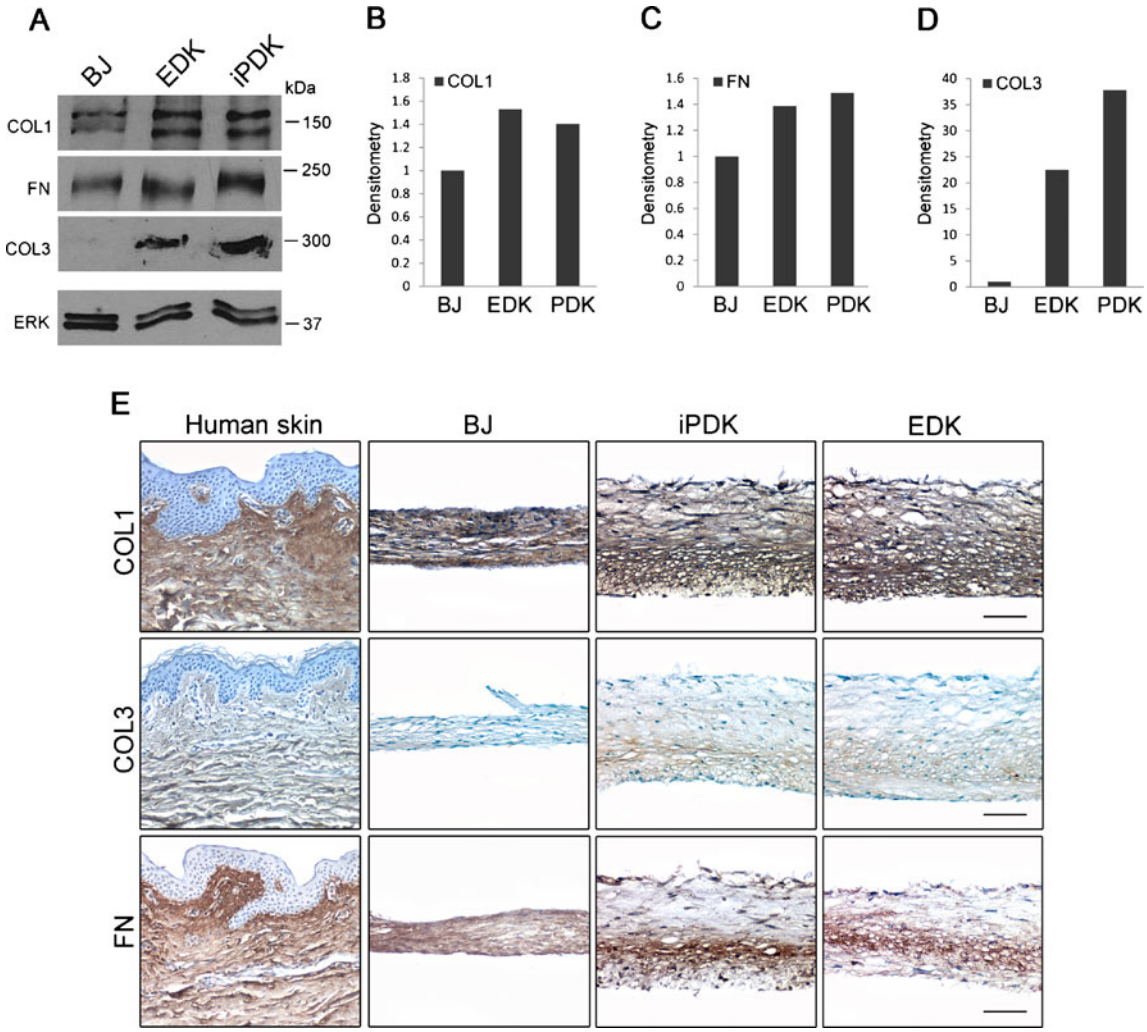

Figure 5. Tissues assembled by hESC- and iPSC-fibroblasts are enriched in type III collagen compared to those assembled by BJ fibroblasts. (*A*) Representative Western blot of type I collagen (*COL1*), type III collagen (*COL3*), and fibronectin (*FN*) within 3D ECM assembled by *BJ*, *iPDK*, and *EDK* fibroblasts after 5 wk of growth in presence of AA. *Bars*, 100 μm. Densitometry analysis of the Western blot showed approximately 40% higher COL1 (*B*) and FN (*C*) within tissues assembled by iPDK and EDK. (*D*) Tissues assembled by EDK and iPDK fibroblasts contained 25-fold and 40-fold higher levels of COL3, respectively, when compared to tissues assembled by BJ fibroblasts. (*E*) Immunohistochemical staining of tissues assembled by *EDK*, *iPDK*, and *BJ* fibroblasts compared to control sections of *Human skin*. *Bars*, 100 μm.

extracellular space (Hata and Senoo 1989). Such stroma-like structures have been defined in previous studies as "self-assembled" or cell-derived ECM (Pouyani et al. 2009; Throm et al. 2010), where fibroblasts deposit and organize an ECM, comprised primarily of type I collagen and fibronectin, that displays features of a provisional matrix seen during the early stages of wound repair (Pouyani et al. 2009). We have found that both, hESC- and iPSC-derived fibroblasts (EDK and iPDK, respectively) were highly responsive to AA, which demonstrates that these cells retain this important functional property of stromal fibroblasts following their differentiation from pluripotent stem cells. For example, when cultured in 2D monolayer culture in the presence of AA, EDK and iPDK fibroblasts increased their expression of collagen genes, secretion of total soluble collagen, and the extracellular deposition of type I collagen to a significantly greater degree than those seen in the parental BJ fibroblasts. When grown in the presence of AA under culture conditions that enabled the organization of a 3D ECM, EDK and iPDK fibroblasts acquired a highly synthetic phenotype that was characterized by elevated ECM production and organization that generated stroma-like tissues that showed significantly greater amounts of ECM than were found to be deposited by parental BJ fibroblasts. The analysis of the composition of these stromal tissues revealed that EDK- and iPDK-harboring tissues contained greater amounts of type III collagen when compared to BJ-harboring tissues, indicating their similarities to

provisional matrix seen during the early stages of wound repair (Namazi et al. 2011). These differences were seen in spite of the morphologic similarities and overlap in expression of CD surface markers that were seen when EDK, iPDK, and parental BJ fibroblasts were grown in 2D culture for up to 5 wk. This phenotypic stability demonstrates that the dramatic changes seen in collagen production in 2D culture and in 3D tissue assembly were not due to changes that occurred in these cells during prolonged culture or upon AA exposure. Taken together, our findings revealing a greater degree of ECM production and assembly and an increased type III collagen deposition in tissues harboring EDK and iPDK fibroblasts when compared to BJ fibroblasts suggests that hESC- and iPSC-derived fibroblasts represent a replenishing source of potent fibroblasts that may be useful for repair of wounds.

Importantly, functional differences between iPSC- and hESC-derived cells and parental, BJ fibroblasts were only fully revealed when these cells were grown in a complex, 3D tissue environment. This suggests that evaluation of the biological potential of iPSC-derived cells will require the development of reliable methods to evaluate their functional properties before they can be translated for human therapy. Such analysis of cell potency is currently limited by the nature of 2D, monolayer cultures that cannot fully evaluate cellular function due to the absence of an vivo-like tissue context. By characterizing the properties of iPSC-derived, differentiated cells using bioengineered 3D tissues as more predictive models of in vivo tissue responses, it will be possible to better assess cellular behaviors before future therapeutic transplantation. Such tissue surrogates can therefore serve as a platform to assess the developmental capacity of iPSC-derived cells to become functional cell types and will enable identification of iPSC-derivatives optimized for future regenerative therapies.

Our findings extend recent studies showing that fibroblasts derived from iPSC acquire phenotypic properties that exceed those of fibroblasts from which they were initially reprogrammed. For example, iPSC-derived fibroblasts display an extended replicative potential (Suhr et al. 2009) and improved mitochondrial function (Suhr et al. 2010) when compared to the parental fibroblasts used to reprogram the iPSC from which they were differentiated. In addition, we recently found that hESC-derived fibroblasts manifest a repair-promoting phenotype following wounding of 3D human skin equivalents (Shamis et al. 2011). Based on these findings, future therapies using iPSC-derived cells may be targeted to improve repair of non-healing wounds. For example, it is known that fibroblasts from non-healing wounds maintain their pathogenic phenotype due to premature senescence (Falanga 2005; Telgenhoff and Shroot 2005), failure to respond to growth factors (Loot et al. 2002; Galkowska et al. 2006), and an inability to recruit cellular precursors needed to direct granulation tissue formation (Telgenhoff and Shroot 2005). During reprogramming to pluripotency, iPSC acquire elongated telomeres, to evade premature replicative senescence (Marion and Blasco 2010). As chronic wounds are recalcitrant to repair due to senescence-mediated cell cycle arrest of wound fibroblasts (Telgenhoff and Shroot 2005), overcoming this senescent phenotype may be important in generating wound repair-competent cells to improve healing. Taken together with our findings of improved growth and ECM production in iPSC-derived fibroblasts, our approach may lay the foundation through which somatic fibroblasts may undergo "recalibration" of their repair phenotype (Suhr et al. 2009; Suhr et al. 2010; Shamis et al. 2011) upon reprogramming to iPSC in a way that can revert fibroblast to a more functional state leading to restoration of tissue health. By comparing the biological potential of iPSC-derived fibroblasts to fibroblasts from which iPSC were originally reprogrammed, we have taken an important step towards understanding how iPSC-derived fibroblasts may demonstrate improved efficacy and function for future regenerative therapies.

Acknowledgments We would like to thank Drs. Nimet Maherali and Konrad Hochedlinger for the BJ-iPSC line and Judith Edwards for help in preparation of this manuscript. This work was supported by grant no. DE017413 to JAG from National Institute for Dental Research (NIDCR).

Conflicts of interest The authors indicate no potential conflicts of interest.

References

Chang H. Y.; Chi J. T.; Dudoit S.; Bondre C.; van de Rijn M.; Botstein D.; Brown P. O. Diversity, topographic differentiation, and positional memory in human fibroblasts. *Proc Natl Acad Sci USA* 99: 12877–12882; 2002.

Chojkier M.; Houglum K.; Solis-Herruzo J.; Brenner D. A. Stimulation of collagen gene expression by ascorbic acid in cultured human fibroblasts. A role for lipid peroxidation? *J Biol Chem* 264: 16957–16962; 1989.

Falanga V. Wound healing and its impairment in the diabetic foot. *Lancet* 366: 1736–1743; 2005.

Galkowska H.; Wojewodzka U.; Olszewski W. L. Chemokines, cytokines, and growth factors in keratinocytes and dermal endothelial cells in the margin of chronic diabetic foot ulcers. *Wound Repair Regen: official publication of the Wound Healing Society [and] the European Tissue Repair Society* 14: 558–565; 2006.

Grainger S. J.; Putnam A. J. Assessing the permeability of engineered capillary networks in a 3D culture. *PLoS One* 6: e22086; 2011.

Gurkan U. A.; Cheng X.; Kishore V.; Uquillas J. A.; Akkus O. Comparison of morphology, orientation, and migration of tendon derived fibroblasts and bone marrow stromal cells on electrochemically aligned collagen constructs. *J Biomed Mater Res A* 94: 1070–1079; 2010.

Haniffa M. A.; Wang X. N.; Holtick U.; Rae M.; Isaacs J. D.; Dickinson A. M.; Hilkens C. M.; Collin M. P. Adult human fibroblasts are potent immunoregulatory cells and functionally equivalent to mesenchymal stem cells. *J Immunol* 179: 1595–1604; 2007.

Hata R.; Senoo H. L-ascorbic acid 2-phosphate stimulates collagen accumulation, cell proliferation, and formation of a three-dimensional tissuelike substance by skin fibroblasts. *J Cell Physiol* 138: 8–16; 1989.

Hewitt K. J.; Shamis Y.; Carlson M. W.; Aberdam E.; Aberdam D.; Garlick J. A. Three-dimensional epithelial tissues generated from human embryonic stem cells. *Tissue Eng Part A* 15: 3417–3426; 2009.

Hewitt K. J.; Shamis Y.; Hayman R. B.; Margvelashvili M.; Dong S.; Carlson M. W.; Garlick J. A. Epigenetic and phenotypic profile of fibroblasts derived from induced pluripotent stem cells. *PLoS One* 6: e17128; 2011.

Klimanskaya I.; Rosenthal N.; Lanza R. Derive and conquer: sourcing and differentiating stem cells for therapeutic applications. *Nat Rev Drug Discov* 7: 131–142; 2008.

Koumas L.; King A. E.; Critchley H. O.; Kelly R. W.; Phipps R. P. Fibroblast heterogeneity: existence of functionally distinct Thy 1 (+) and Thy 1(−) human female reproductive tract fibroblasts. *Am J Pathol* 159: 925–935; 2001.

Lapasset L.; Milhavet O.; Prieur A.; Besnard E.; Babled A.; Ait-Hamou N.; Leschik J.; Pellestor F.; Ramirez J. M.; De Vos J.; Lehmann S.; Lemaitre J. M. Rejuvenating senescent and centenarian human cells by reprogramming through the pluripotent state. *Genes Dev* 25: 2248–2253; 2011.

Lian Q.; Lye E.; Suan Yeo K.; Khia Way Tan E.; Salto-Tellez M.; Liu T. M.; Palanisamy N.; El Oakley R. M.; Lee E. H.; Lim B.; Lim S. K. Derivation of clinically compliant MSCs from CD105+, CD24-differentiated human ESCs. *Stem Cells* 25: 425–436; 2007.

Lian Q.; Zhang Y.; Zhang J.; Zhang H. K.; Wu X.; Lam F. F.; Kang S.; Xia J. C.; Lai W. H.; Au K. W.; Chow Y. Y.; Siu C. W.; Lee C. N.; Tse H. F. Functional mesenchymal stem cells derived from human induced pluripotent stem cells attenuate limb ischemia in mice. *Circulation* 121: 1113–1123; 2010.

Liu H.; Kim Y.; Sharkis S.; Marchionni L.; Jang Y. Y. In vivo liver regeneration potential of human induced pluripotent stem cells from diverse origins. *Sci Transl Med* 3: 82ra39; 2011.

Loot M. A.; Kenter S. B.; Au F. L.; van Galen W. J.; Middelkoop E.; Bos J. D.; Mekkes J. R. Fibroblasts derived from chronic diabetic ulcers differ in their response to stimulation with EGF, IGF-I, bFGF and PDGF-AB compared to controls. *Eur J Cell Biol* 81: 153–160; 2002.

Maherali N.; Ahfeldt T.; Rigamonti A.; Utikal J.; Cowan C.; Hochedlinger K. A high-efficiency system for the generation and study of human induced pluripotent stem cells. *Cell Stem Cell* 3: 340–345; 2008.

Marion R. M.; Blasco M. A. Telomeres and telomerase in adult stem cells and pluripotent embryonic stem cells. *Adv Exp Med Biol* 695: 118–131; 2010.

Murad S.; Grove D.; Lindberg K. A.; Reynolds G.; Sivarajah A.; Pinnell S. R. Regulation of collagen synthesis by ascorbic acid. *Proc Natl Acad Sci USA* 78: 2879–2882; 1981.

Namazi M. R.; Fallahzadeh M. K.; Schwartz R. A. Strategies for prevention of scars: what can we learn from fetal skin? *Int J Dermatol* 50: 85–93; 2011.

Peterkofsky B. The effect of ascorbic acid on collagen polypeptide synthesis and proline hydroxylation during the growth of cultured fibroblasts. *Arch Biochem Biophys* 152: 318–328; 1972.

Phan S. H. Biology of fibroblasts and myofibroblasts. *Proc Am Thorac Soc* 5: 334–337; 2008.

Pouyani T.; Ronfard V.; Scott P. G.; Dodd C. M.; Ahmed A.; Gallo R. L.; Parenteau N. L. De novo synthesis of human dermis in vitro in the absence of a three-dimensional scaffold. In vitro cellular & developmental biology. *Animal* 45: 430–441; 2009.

Proulx S.; d'Arc Uwamaliya J.; Carrier P.; Deschambeault A.; Audet C.; Giasson C. J.; Guerin S. L.; Auger F. A.; Germain L. Reconstruction of a human cornea by the self-assembly approach of tissue engineering using the three native cell types. *Mol Vis* 16: 2192–2201; 2010.

Schmidt D.; Hoerstrup S. P. Tissue engineered heart valves based on human cells. *Swiss Med Wkly* 136: 618–623; 2006.

Schultz G. S.; Wysocki A. Interactions between extracellular matrix and growth factors in wound healing. *Wound Repair Regen: official publication of the Wound Healing Society [and] the European Tissue Repair Society* 17: 153–162; 2009.

Shamis Y.; Hewitt K. J.; Carlson M. W.; Margvelashvilli M.; Dong S.; Kuo C. K.; Daheron L.; Egles C.; Garlick J. A. Fibroblasts derived from human embryonic stem cells direct development and repair of 3D human skin equivalents. *Stem Cell Res Ther* 2: 10; 2011.

Sorrell J. M.; Baber M. A.; Caplan A. I. Clonal characterization of fibroblasts in the superficial layer of the adult human dermis. *Cell Tissue Res* 327: 499–510; 2007.

Sorrell J. M.; Baber M. A.; Caplan A. I. Human dermal fibroblast subpopulations; differential interactions with vascular endothelial cells in coculture: nonsoluble factors in the extracellular matrix influence interactions. *Wound Repair Regen: official publication of the Wound Healing Society [and] the European Tissue Repair Society* 16: 300–309; 2008.

Sorrell J. M.; Caplan A. I. Fibroblast heterogeneity: more than skin deep. *J Cell Sci* 117: 667–675; 2004.

Sottile J.; Shi F.; Rublyevska I.; Chiang H. Y.; Lust J.; Chandler J. Fibronectin-dependent collagen I deposition modulates the cell response to fibronectin. *Am J Physiol Cell Physiol* 293: C1934–C1946; 2007.

Stojkovic P.; Lako M.; Stewart R.; Przyborski S.; Armstrong L.; Evans J.; Murdoch A.; Strachan T.; Stojkovic M. An autogeneic feeder cell system that efficiently supports growth of undifferentiated human embryonic stem cells. *Stem Cells* 23: 306–314; 2005.

Suhr S. T.; Chang E. A.; Rodriguez R. M.; Wang K.; Ross P. J.; Beyhan Z.; Murthy S.; Cibelli J. B. Telomere dynamics in human cells reprogrammed to pluripotency. *PLoS One* 4: e8124; 2009.

Suhr S. T.; Chang E. A.; Tjong J.; Alcasid N.; Perkins G. A.; Goissis M. D.; Ellisman M. H.; Perez G. I.; Cibelli J. B. Mitochondrial rejuvenation after induced pluripotency. *PLoS One* 5: e14095; 2010.

Swistowski A.; Peng J.; Liu Q.; Mali P.; Rao M. S.; Cheng L.; Zeng X. Efficient generation of functional dopaminergic neurons from human induced pluripotent stem cells under defined conditions. *Stem Cells* 28: 1893–1904; 2010.

Telgenhoff D.; Shroot B. Cellular senescence mechanisms in chronic wound healing. *Cell Death Differ* 12: 695–698; 2005.

Thomson J. A.; Itskovitz-Eldor J.; Shapiro S. S.; Waknitz M. A.; Swiergiel J. J.; Marshall V. S.; Jones J. M. Embryonic stem cell lines derived from human blastocysts. *Science* 282: 1145–1147; 1998.

Throm A. M.; Liu W. C.; Lock C. H.; Billiar K. L. Development of a cell-derived matrix: effects of epidermal growth factor in chemically defined culture. *J Biomed Mater Res A* 92: 533–541; 2010.

Wong T.; McGrath J. A.; Navsaria H. The role of fibroblasts in tissue engineering and regeneration. *Br J Dermatol* 156: 1149–1155; 2007.

Xu C.; Jiang J.; Sottile V.; McWhir J.; Lebkowski J.; Carpenter M. K. Immortalized fibroblast-like cells derived from human embryonic stem cells support undifferentiated cell growth. *Stem Cells* 22: 972–980; 2004.

Yamaguchi Y.; Itami S.; Tarutani M.; Hosokawa K.; Miura H.; Yoshikawa K. Regulation of keratin 9 in nonpalmoplantar keratinocytes by palmoplantar fibroblasts through epithelial-mesenchymal interactions. *J Invest Dermatol* 112: 483–488; 1999.